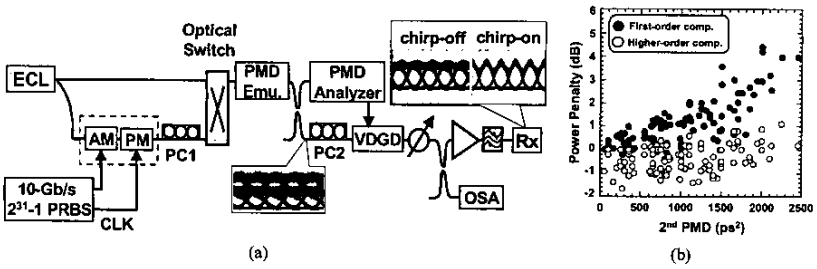

WQ1 Fig. 2. Higher-order PMD compensation using emulator that consists of 30-section PM fiber. (a) Experimental setup (b) First-order and higher-order compensation results as a function of the second-order PMD.

random polarization states for the first-order PMD compensation case.

4. Simulation Results

PMD compensation is modeled for NRZ 40-Gb/s transmission over a fiber link that has Maxwellian PMD statistics.[1] The link is modeled by 25 cascaded segments, each having a randomly distributed DGD (Maxwellian) and a randomly oriented PSP (uniform on the Poincaré sphere). We assume chromatic dispersion and fiber nonlinearities do not accumulate along the link since we are trying to isolate the effect of PMD separately. The PMD-induced Q-factor penalty for each fiber sample is calculated from the simulated BER versus the receiver decision threshold, assuming that amplified spontaneous emission (ASE) is the dominant noise source. First-order PMD compensation is achieved by compensating the link DGD to exactly zero at the signal spectral center, and the signal input SOP is controlled by a feedback loop of two control variables to maximize the simulated eye opening.

The purpose of PMD compensation is to reduce the probability of inducing large system penalties or link outages due to PMD. Under the assumption that an outage occurs when the Q-penalty is greater than 2.5 dB, Fig. 3(a) shows the outage probability as a function of the average DGD for an ensemble of independent fiber samples. Simulations show that, similar to first-order PSP transmission, the feedback loop controlling the input SOP does not suffer from the local-optima. As a result, the outage probability calculated using a local optimization algorithm (open circles in Fig. 3a) basically agrees with the probability calculated from a global optimization of input SOP over the whole Poincare sphere (solid circles). According to the criterion of the outage probability of 1/18,000, the system tolerance to PMD can be increased from 7.5 ps after first-order compensation to 10 ps after higher-order compensation. The Q penalty distributions for both first-order and higher-order compensation at 12.5-ps average PMD are shown in Fig. 3(b).

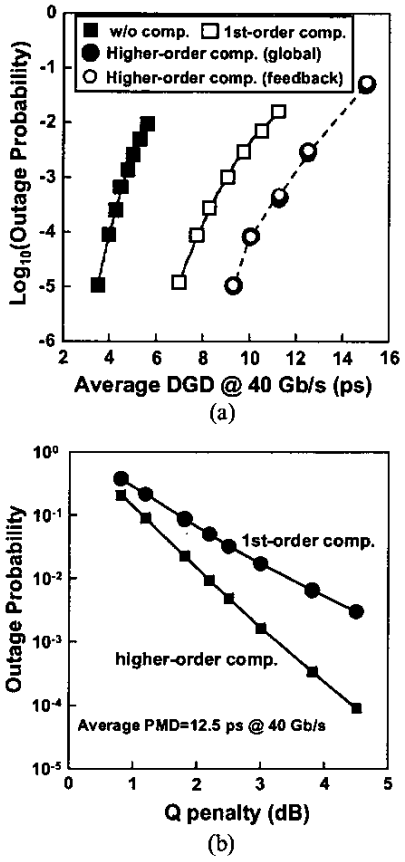

WQ1 Fig. 3. Simulation results for 40-Gb/s NRZ transmission (a) Probability of Q-penalties exceeding 2.5 dB, here for the higher-order compensation, the open circles is calculated from the compensation based on feedback control and the solid circle is based on global optimization. (b) Outage probability as a function of Q penalty for first-order compensation and higher-order compensation with 12.5-ps link average PMD.

References

1. C.D. Poole, and J. Nagel, *Optical Fiber Telecommunications,* San Diego: Academic, vol. III-A, chapter 6, pp. 114–161, (1997).
2. R.M. Jopson, L.E. Nelson, G.J. Pendock, A.H. Gnauck, "Polarization-mode dispersion impairment in return-to-zero and nonreturn-to-zero systems," OFC '99, paper WE3, (1999).
3. F. Heismann, D.A. Fishman, and D.L. Wilson, "Automatic compensation of first-order polarization mode dispersion in a 10 Gb/s transmission system," ECOC '98, 529–530, (1998).
4. H. Bülow, "Limitation of Optical First-order PMD Compensation," OFC '99, paper WE1, (1999).
5. Q. Yu, L.-S. Yan, Y. Xie, M. Hauer and A.E. Willner, "Higher order polarization mode dispersion compensation using a fixed time delay followed by a variable time delay," IEEE Photonics Technol. Lett., 8, 863–865, (2001).
6. M. Shtaif, A. Mecozzi, M. Tur, and J.A. Nagel, "A Compensator for the Effects of High-Order Polarization Mode Dispersion in Optical Fibers," IEEE Photonics Technol. Lett., 12, 434–435, (2000).
7. R. Noé, D. Sandel, M. Yoshida-Dierolf, S. Hinz, et al. "Polarization mode dispersion compensation at 10, 20, and 40 Gb/s with various optical equalizers," J. of Lightwave Technol., 17, 1602–1616, (1999).
8. T. Ono, Y. Yano, L.F. Garrett, J.A. Nagel, M.J. Dickerson and M. Cvijetic, "10 Gb/s PMD compensation field experiment over 452 km using principal state transmission method," OFC '2000, paper PD44, (2000).
9. William Shieh, "On the Second-Order Approximation of PMD," IEEE Photonics Technol. Lett, 12, 290–292, (2000).

WQ2 **4:15 pm**

Coherent heterodyne frequency-selective polarimeter for error signal generation in higher-order PMD compensators

I. Roudas, *Corning Inc., 2200 Cottontail Ln., Somerset, NJ 0887, USA. Tel. (732) 748-3716. Email: roudasj@corning.com*

G. Piech, M. Mlejnek, Y. Zhu, and D.Q. Chowdhury, *Corning Inc., Corning, NY 14831, USA*

1. Introduction

Polarization-mode dispersion (PMD) is a major impairment for the achievement of ultra-high capacity transmission over installed legacy optical fibers. For this purpose, several optical and electronic adaptive PMD compensation schemes are proposed in the bibliography.[1–7] All aforementioned techniques comprise a form of PMD monitoring device, which generates an error signal for driving the control unit of the adaptive PMD compensator. Frequency-selective polarimeters, i.e., devices which can measure the variation of Stokes parameters as a function of frequency,[6,8,9] are especially attractive candidates for PMD monitoring in higher-order PMD compensators because frequency-resolved Stokes parameters can provide, at least in principle, information about all PMD orders.

In this article we propose a novel coherent heterodyne receiver architecture, which can operate as a frequency-selective polarimeter. An original and efficient algorithm is used for the estimation of the Stokes parameters of the received signal spectrum. We demonstrate the operation of the coherent receiver by measuring the Stokes parameters of a 10 Gb/s NRZ signal after propagation through a polarization-maintaining (PM) fiber. To illustrate the potential use of the coherent heterodyne receiver as PMD monitoring device in adaptive PMD compensators, we generate

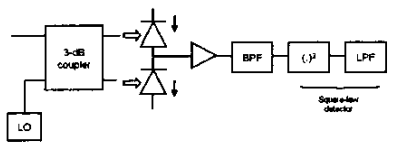

WQ2 Fig. 1. Schematic of coherent heterodyne polarimeter. (Symbols: BPF = Bandpass filter, $(\cdot)^2$ = Square-law device (microwave mixer), LPF = Lowpass filter).

an error signal, similar to the one proposed by,[6] from the frequency-resolved Stokes parameters of the received signal, and study its properties in the presence of first- and higher-order PMD.

2. Operating principle of the coherent heterodyne receiver

Fig. 1 shows the block diagram of the coherent heterodyne receiver. It is composed of a local oscillator (LO), a 3-dB coupler, a balanced receiver front-end consisting of two identical pin photodiodes and an electronic preamplifier, a bandpass filter (BPF), and a square-law detector consisting of a microwave mixer and a lowpass filter (LPF).

The photocurrent at the output of an ideal balanced receiver front-end originates exclusively from coherent detection, i.e., the beating between the received optical signal and the local oscillator.[10] The coherent detection spectrum is centered at the frequency difference between the source and the local oscillator (intermediate frequency f_{IF}). The intermediate frequency can be varied by tuning the frequency of the local oscillator. A narrow-band BPF is used to cut a very thin slice of the modulated signal spectrum around the BPF center frequency f_c (not necessarily equal to intermediate frequency f_{IF}). The rest of the receiver is used to measure the power of this spectral slice. It will be shown below that the power of the spectral slice can be used to estimate the SOP of the received signal at the vicinity of frequency f_c.

It is possible to analytically calculate the photocurrent at the output of the coherent receiver in the case when both the received signal and the local oscillator are planar monochromatic waves:

$$i_{LPF} = R^2 P_s P_{lo}(1 + \hat{e}_s \hat{e}_{lo}) \qquad (1)$$

where R is the responsivity of the photodiodes, P_s, P_{lo} are the average powers of the received signal and local oscillator respectively, and $\hat{e}_s$, $\hat{e}_{lo}$ are normalized Stokes vectors corresponding to the SOPs of the received signal and local oscillator respectively.

Using (1), first it is possible to estimate the factor $R^2 P_s P_{lo}$, from two measurements of the photocurrent corresponding to two antiparallel (in Stokes space) local oscillator SOPs. Then, the Stokes components of the signal (S_x, S_y, S_z) can be evaluated based on three different measurements of the photocurrent $i_{LPF}|_k$ corresponding to three non-coplanar local oscillator SOPs with known Stokes components ($S_x^{(k)}$, $S_y^{(k)}$, $S_z^{(k)}$), k = 1, . . . 3, through the set of equations:

$$\begin{pmatrix} S_x^{(1)} & S_y^{(1)} & S_z^{(1)} \\ S_x^{(2)} & S_y^{(2)} & S_z^{(2)} \\ S_x^{(3)} & S_y^{(3)} & S_z^{(3)} \end{pmatrix} \begin{pmatrix} S_x \\ S_y \\ S_z \end{pmatrix} = \frac{1}{R^2 P_s P_{lo}} \begin{pmatrix} i_{LPF}|_{(1)} \\ i_{LPF}|_{(2)} \\ i_{LPF}|_{(3)} \end{pmatrix} - 1 \qquad (2)$$

The simplest solution of the above set of equations is obtained for local oscillator SOP settings k = 1, . . . ,3 corresponding to linear 0 deg, linear 45 deg and right- or left-circular polarization. Such a choice makes the 3 × 3 matrix in the LHS of (2) unity for a right- or left-circular Stokes space respectively.

In the case of modulated received signal, the above analysis is most accurate if the BPF bandwidth is infinitesimal and is approximate otherwise. The estimation of the variation of Stokes parameters of the received modulated signal as a function of frequency involves several steps: i) Tuning of the frequency of the local oscillator at closely spaced intervals, within the signal bandwidth; ii) At each frequency, changing the local oscillator SOP between three known SOPs and measuring the corresponding photocurrents at the output of the coherent heterodyne receiver; iii) Solution of the set of equations (2) for each frequency.

3. Error signal generation

Several error signals can be generated from the frequency-resolved Stokes parameters provided by the coherent heterodyne receiver. The choice of the most adequate error signal form depends on several criteria, e.g., order of desired PMD compensation, monotonicity of the error signal as a function of power penalty in order to achieve a desired error probability, and so forth. For illustration purposes, we study the properties of an error signal, similar to the one proposed by,[6] defined here as the sum of the variances of the frequency-resolved Stokes parameters across a measurement window Δf (frequency scanning range).

In the case when first-order PMD is dominant, it is possible to derive an analytical relationship for the aforementioned error signal as a function of differential group delay (DGD) τ[11] and the power splitting ratio γ between the x- and y-polarizations:

$$\varepsilon = 4\gamma(1-\gamma)\left[1 - \frac{\sin(\pi\tau\Delta f)^2}{(\pi\tau\Delta f)^2}\right] \qquad (3)$$

Expression (3) shows that the error signal depends on the frequency scanning range. For $\Delta f\tau < 1$, the error signal is monotonic but it saturates for $\Delta f\tau = 1$ and presents oscillations for $\Delta f\tau > 1$. For a completely monotonic signal we require $\Delta f\tau \leq 1$. The amplitude of the error signal is maximum for $\gamma = 0.5$ and decreases for all other values of γ. The shape of the curves is independent of γ.

4. Case study: frequency-resolved Stokes parameters detection and error signal generation

For experimental convenience, the tests to verify and evaluate the above concepts differed from the above theoretical description in two regards. First, we used only a single photodiode, rather than a balanced receiver. Second, instead of scanning the frequency of the local oscillator, we held the local oscillator frequency constant and scanned the BPF center frequency across the heterodyne spectrum by using an RF spectrum analyzer. The signal beam was at 1559.79 nm, was modulated with a 2^{31} PRBS sequence at 10 Gb/s, had a power at the receiver of –20 dBm, and an optical signal-to-noise ratio (OSNR) above 40 dB, measured in a resolution bandwidth 0.1 nm. The local oscillator power at the receiver was –0.5 dBm, its SOP was commanded to distinct states by an electro-optic polarization controller, and these SOPs were recorded using a tap and polarimeter. A controlled amount of first-order PMD was introduced in the system using a JDS (PE-3) PMD emulator. Data was acquired for a frequency scanning range of 15 GHz, with a spectrum analyzer resolution bandwidth of 3 MHz and video bandwidth of 30 kHz. Results for 50 ps of DGD are shown in Fig. 2. They clearly exhibit the sinusoidal oscillations expected for first-order PMD. In addition, to evaluate the accuracy of (3), measurements of the error signal were made for DGD ranging from 0–100 ps. As shown in Fig. 3(a), equation (3) fits well the experimental data for $\gamma = 0.29$.

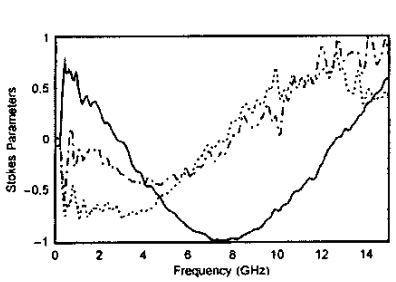

WQ2 Fig. 2. Normalized Stokes parameters measured by the coherent heterodyne receiver in a scanning window of 15 GHz for DGD equal to half the bit period.

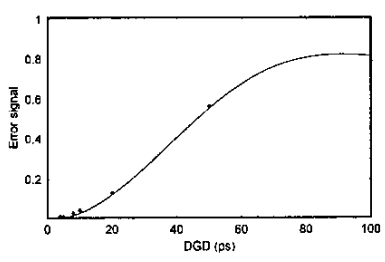

3(a)

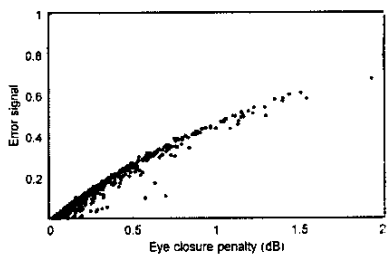

3(b)

WQ2 Fig. 3. (a) Error signal vs. DGD for a 10 Gb/s system. (Symbols: Points = measurements, line = expression (3) with $\gamma = 0.29$). (b) Simulated error signal vs. eye closure penalty for a 40 Gb/s RZ signal, with all orders of PMD present.

Finally, the sensitivity of the error signal to all orders of PMD was studied by simulation. For this purpose, a 40 Gb/s RZ noiseless signal was transmitted through a 100 km long fiber, with average DGD of about 6 ps, modeled as a concatenation of identical randomly-oriented birefringent waveplates. All other fiber impairments were neglected. In Fig. 3(b), the error signal is plotted versus the PMD induced eye-closure penalty, for 1000 realizations of fiber birefringence orientation. It is observed that the presence of higher-order PMD destroys the strict monotonicity of the error signal. Results on the generation of more robust error signals will be presented at the conference.

5. Summary

We proposed and demonstrated a coherent heterodyne receiver architecture that can frequency-resolve the Stokes parameters of a modulated signal. We also studied the feasibility of generation of an error signal based on the Stokes parameters variance. We presented experimental results for a 10 Gb/s NRZ signal with first-order PMD and theoretical results for a 40 Gb/s RZ signal with higher-order PMD.

References

1. T. Ono, S. Yamazaki, H. Shimizu, K. Emura, *J. Lightwave Tech.*, vol. 12, No. 5, May 1994, pp. 891–898.
2. T. Takahashi, T. Imai, and M. Aiki, *Electron. Lett.*, vol. 30, pp. 348–349, 1994.
3. B.W. Hakki, *IEEE Photonics Tech. Lett.*, vol. 9, No. 1, pp. 121–123, Jan. 1997.
4. F. Heismann, D.A. Fishman, and D.L. Wilson, *Proc. ECOC '98*, Madrid, Spain, 1998, pp. 529–530.
5. D. Sandel, M. Yoshida-Dierolf, R. Noe, A. Schopflin, E. Gottwald, and G. Fischer, *El. Lett.*, Vol. 34, No. 23, pp. 2258–2259, Nov. 1998.
6. H. Rosenfeldt, R. Ulrich, U. Feiste, R. Ludwig, H.G. Weber, and A. Ehrhardt, *El. Lett.*, Vol. 36, No. 5, pp. 448–450, Mar. 2000.
7. C. Francia, F. Bruyere, J.P. Thiery, and D. Penninckx, *El. Lett.*, Vol. 35, No. 5, pp. 414–415, Mar. 1999.
8. L. Möller and L. Buhl, *J. Lightwave Tech.*, Vol. 19, pp. 1125–1129, Aug. 2001.
9. S. Shin, I. Yeo, H. Song, J. Park, Y. Park, and B. Jo, Proc. *OFC '01*, paper TuP7, Anaheim, CA, USA, Mar. 2001.
10. R.A. Linke and A.H. Gnauck, *J. Lightwave Tech.*, Vol. 5, pp. 1750–1769, Nov. 1988.
11. C.D. Poole and R.E. Wagner, *Electron. Lett.*, Vol. 22, No. 19, pp. 1029–1030, Sep. 1986.

WQ3 **4:30 pm**

Improvement of first-order optical PMD compensator by relevant control of input state of polarization

E. Corbel, S. Lanne and J-P. Thiéry, *Alcatel Research & Innovation, Route de Nozay, 91460 Marcoussis, France, Email: erwan.corbel@ms.alcatel.fr*

1. Introduction

Due to manufacturing inhomogeneities and external stresses in fibers, degeneracy between the two modes of propagation vanishes and leads to an unwanted birefringence which varies along the fiber.[1] Polarization-Mode Dispersion (PMD) applies to a modulated signal and accounts for the frequency dependence of the polarization state of its spectral components. In a first-order approach in frequency, a modulated signal is depolarized unless its input state of polarization (ISOP) is along one of two preferential vectors on the Poincaré sphere: the Principal States of Polarization (PSP). Because of different group velocities along the two PSP, the two components of an input along the directions of PSP are shifted in time by the Differential Group Delay (DGD) after propagating. Thus PMD brings about signal distortions which cause system impairments in a statistical way. PMD stochastic nature lies in the time dependence of the local birefringence. Furthermore, due to frequency dependence of birefringence, one must overtake this first-order frame of work in order to be more realistic and take into account the DGD and PSP variations with frequency respectively called Polarization-dependent Chromatic Dispersion (PCD) and depolarization (2k).[2]

The higher the bit-rate, the more deleterious the impact of PMD. In the perspective of systems operating at 40 Gb/s, some new low-PMD fibers have been considered. Operators resort to PMD compensation techniques in order to improve the PMD tolerance of their networks. Among all the means to mitigate PMD,[3] optical compensators have the major advantage to be independent of bit-rate.[4] This scalability enables us to extrapolate the results obtained at 10 Gb/s to 40 Gb/s. In this paper, we focus on the improvement of a first-order PMD mitigator running thanks to a slow control of input state of polarization. We performed simulations and experiments in order to assess the efficiency of our scheme.

2. Principle

A two-degree of freedom mitigator,[5] consists of a polarization controller (PC), followed by a polarization-maintaining fiber (PMF) with a fixed DGD. A feedback loop enables us to cope with the statistical nature of PMD, facing any variations of external conditions (see Figure 1). The feedback signal must be chosen as a trade-off between sensitivity, response time and its correlation with BER.[3] In our case, the degree of polarization (DOP) is used. It is insensitive to bit-rate and well correlated with BER. Thanks to such a mitigator, the tolerable PMD value, that is to say the mean value of the stochastic parameter DGD which allows to keep the sensitivity penalty under 3 dB except for 0.001% of the time, is increased from 15 to 30% of the bit-time.[4] One of the limitations of this compensator is the presence of a sub-optimum of the feedback signal.[6] What is more, we know that PMD dynamics can make PMD conditions last up to a day.[7]

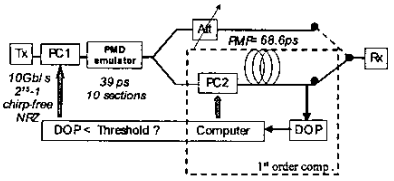

WQ3 Fig. 1. Set-up of the scheme of compensation with ISOP control.

Many compensators with more than two degrees of freedom have been proposed. Some of them separate first and second-order compensation[8,9] but remain difficult to implement in spite of their efficiency. Some others use post-compensation with two stages but one feedback signal.[10] It brings a slight improvement in comparison with simple compensator. Otherwise a compensator with two feedback signals[5] have been proposed and seems to be worthy despite the growth of complexity in feedback algorithm. In all cases, this type of post-compensators do not meet cost requirements of systems designers because of the necessity of two fast polarization controllers.

The purpose of our new scheme of compensation would be to overcome a deleterious stagnation on a sub-optimum. Its principle lies in the change of the function $DOP(\Omega_C)$ (where Ω_C is the PMD vector of the compensator), the one that exhibits a sub-optimum, thanks to ISOP control. The set-up is shown in Figure 1. It resorts to ISOP control only if the first-order compensator leads to a value of feedback signal below a threshold which depends on the installed system. If so, the ISOP is modified thanks to a polarization controller before the line. This operation is repeated several times. In fact the aim of ISOP control is to provide a slow and step-by-step optimization of feedback signal similar to the one performed by first-order compensator. Moreover the variation of the ISOP must be fine so as to preserve the quality of the transmission. Even if it needs the use of a feedback loop across the line of transmission, this feedback is slow (a fast polarization controller is not required) and triggered unlike the PSP alignment methods. Note that our scheme differs from polarization scrambling because it leads to an ISOP selection.

3. Experimental verifications

Experimental set-up is depicted on Figured 1. Our emulator consists of 10 sections of couple {PC + PMF}. PMD conditions changes and all the parameter measurements (e.g., BER and DOP) we are interested in are fully automatically carried out by our testing bench.[4] The PMD of the emulator is 39 ps. 2000 draws of PMD conditions were considered. The DGD of the compensator is optimized in function of the PMD value in the emulator.

Figure 2-a shows the cumulative probability function for power sensitivity penalty due to PMD (it addresses the probability to be above a given value of the penalty) without any compensation, with compensation based on first-order mitigator and with compensation using ISOP control in addition of first-order mitigator. The sensitivity penalty is obtained by a translation of measured BER into receiver sensitivity using a pre-characterization of the pre-amplified reception equipment. It shows the improvement brought by the compensation with ISOP control even if our statistical range is limited to a probability of 10^{-2}. Furthermore the curve corresponding to the transient state during ISOP moving and PC2 fine-tuning (see Figure 1) demonstrates the capability to keep the system efficient at all times.

4. Simulation results

We have performed 2000 simulations on the same set-up as experiments. Figure 2-b shows the cumulative probability function of power sensitivity penalty without any compensation, with com-